



Research Report

การศึกษาสมบัติของบอร์ฟีนสำหรับก๊าซเซนเซอร์ตรวจจับก๊าซพิษ ในสิ่งแวดล้อม

Investigation on Borophene Properties for Toxin Gas Sensors in
Environment

Kriengkri Timsorn

Division of Physics, Faculty of Science and Technology, Phetchabun
Rajabhat University

Full Research Report

การศึกษาสมบัติของบอร์ฟีนสำหรับก๊าซเชนเซอร์ตรวจวัดก๊าซพิษ ในสิ่งแวดล้อม

Investigation on Borophene Properties for Toxin Gas Sensors in Environment

Kriengkri Timsorn

Division of Physics, Faculty of Science and
Technology, Phetchabun Rajabhat
University

Dumrongsak Rodphothong

Department of Physics, Faculty of Science,
Ramkhamhaeng University

Research Scholarship Support for Development of Science, Research and
Innovation

ชื่องานวิจัย	การศึกษาสมบัติของบีโโรฟีนสำหรับก๊าซไฮโดรเจนเชอร์ตัวจับก๊าซพิชในสิ่งแวดล้อม
ผู้วิจัย	ผู้ช่วยศาสตราจารย์ ดร.เกรียงไกร ทิมศรี
ผู้ร่วมวิจัย/ที่ปรึกษา	ผู้ช่วยศาสตราจารย์ ดร.ดำรงศักดิ์ รอดโพธิ์ทอง
สาขาวิชา	พลังงาน

มหาวิทยาลัยราชภัฏเพชรบูรณ์ ปีเสรีจิจัย 2567

บทคัดย่อ

งานวิจัยนี้มุ่งเน้นการศึกษาทางทฤษฎีของหมุดค่อนต้มบีโโรฟีนสำหรับการประยุกต์ใช้เป็นวัสดุตรวจจับโมเลกุลก๊าซของไฮโดรเจนเชอร์ตัวจับก๊าซพิช โดยได้ทำการศึกษาพฤติกรรมการดูดซับของก๊าซ NO_2 , CO_2 , CO และ NH_3 บนโครงสร้างวงล้อไอออนของหมุดค่อนต้มบีโโรฟีนทั้งแบบไม่เติมและแบบที่มีการเติมไนโตรเจน โดยใช้วิธีการคำนวณทางค่อนต้มด้วยเทคนิค SCC-DFTB ในกรณีนี้เทคนิค SCC-DFTB ถูกนำมาใช้ในการตรวจสอบโครงสร้างทางเรขาคณิต จุดดูดซับที่เหมาะสมที่สุด การถ่ายโอนประจุ ความหนาแน่นของสถานะรวม และคุณสมบัติทางอิเล็กทรอนิกส์ของโครงสร้างหมุดค่อนต้มบีโโรฟีนก่อนและหลังการดูดซับก๊าซ ผลการศึกษาพบว่าการเติมไนโตรเจนช่วยปรับปรุงสมบัติการดูดซับก๊าซพิชของหมุดค่อนต้มบีโโรฟีนอย่างมีนัยสำคัญ ทำให้มีความแข็งแรงของอันตรกิริยากับโมเลกุลก๊าซเพิ่มขึ้น การถ่ายโอนประจุที่มากขึ้น และความสามารถในการดัดเลือกก๊าซพิชที่ดีขึ้น นอกจากนี้ การลดของว่างพลังงานหลังการดูดซับก๊าซยังคงบ่งชี้ถึงการนำไฟฟ้าที่เพิ่มขึ้น ซึ่งสนับสนุนถึงศักยภาพของหมุดค่อนต้มบีโโรฟีนสำหรับการใช้งานเป็นเซนเซอร์ตัวจับก๊าซพิช การเติมไนโตรเจนในหมุดค่อนต้มบีโโรฟีนแสดงให้เห็นถึงประสิทธิภาพที่ยอดเยี่ยมในการประยุกต์ใช้เป็นวัสดุตรวจจับโมเลกุลก๊าซของไฮโดรเจนเชอร์ตัวจับก๊าซพิชในสิ่งแวดล้อม โดยเฉพาะการตรวจจับก๊าซ CO_2

คำสำคัญ: บีโโรฟีน ก๊าซไฮโดรเจนเชอร์ตัวจับก๊าซพิช ตรวจจับก๊าซพิช SCC-DFTB

Research Title	Investigation on Borophene Properties for Toxin Gas Sensors in Environment
Investigator	Assistant Professor Dr. Kriengkri Timsorn
Co-Investigator/Mentor	Assistant Professor Dr. Dumrongsak Rodphothong
Branch	Physics
	Phetchabun Rajabhat University year 2024

ABSTRACT

This research focuses on the theoretical investigation of borophene quantum dots (BQDs) for toxic gas sensing applications. The adsorption behaviors of NO_2 , CO_2 , CO and NH_3 on B_9^- wheel structures of pristine and nitrogen functionalized BQDs using the self-consistent charge density functional tight-binding (SCC-DFTB) method were studied. The SCC-DFTB method was performed to investigate structural geometries, the most favorable adsorption sites, charge transfer, total densities of states and electronic properties of the structures before and after adsorption of the gas molecules. The study found that nitrogen functionalization significantly improved the adsorption properties of the BQDs, resulting in enhanced interaction strength, higher charge transfer, and better selectivity for toxic gases. Moreover, the reduction in energy gaps after adsorption suggests increased conductivity that supports the potential of BQDs for use in high-performance gas sensors. Nitrogen functionalization on BQDs demonstrated excellent performance as a sensing material for hazardous environmental gases, particularly CO_2 .

Keywords: borophene, gas sensor, nanomaterial, toxic gas detection, SCC-DFTB

ACKNOWLEDGEMENTS

This research was financially supported by research scholarship support for the development of science, research, and innovation in 2024 (TSRI2567/45).

Kriengkri Timsorn

February 17, 2025

TABLE OF CONTENTS

	Page
THAI ABSTRACT	i
ENGLISH ABSTRACT	ii
ACKNOWLEDGEMENTS	iii
LIST OF TABLES	vi
LIST OF FIGURES	vii
CHAPTER 1 INTRODUCTION	1
1.1 Background and Significance	1
1.2 Objectives	3
1.3 Scope of Research	4
CHAPTER 2 LITERATURE REVIEW	5
CHAPTER 3 METHODOLOGY	14
3.1 Structures of Borophene Quantum Dots (BQDs)	14
3.2 Three-Dimensional Models of Toxic Gas Sensing	15
3.3 Self-Consistent Charge Density Functional Tight-Binding (SCC-DFTB)	16
CHAPTER 4 RESULTS AND DISCUSSION	20
4.1 Structural and Electronic Properties of B_9^- and N/B_9^- BQDs	20
4.2 Adsorption of NO_2 , CO_2 , CO and NH_3 gas molecules on B_9^- BQDs	23
4.3 Adsorption of NO_2 , CO_2 , CO and NH_3 gas molecules on N/B_9^- BQDs	26

4.4	Total Densities of State (DOS)	29
CHAPTER 5	CONCLUSION	31
REFERENCES		33
CURRICULUM VITAE		36

LIST OF TABLES

Table		Page
4-1	Electronic parameter of B_9^- and N/B_9^- BQDs	22
4-2	Typical calculated adsorption parameters for each gas molecule absorbed on the B_9^- BQD structures.	25
4-3	Typical calculated adsorption parameters for each gas molecule absorbed on the N/B_9^- BQD structures	28

LIST OF FIGURES

Figure	Page
2-1 Different structures of borophene	5
2-2 The β -12 structure of borophene	6
2-3 Honeycomb borophene	7
2-4 2-Pmmn borophene	8
3-1 Wheel structures of (a) pristine (B_9^-) and (b) nitrogen functionalized (N/B_9^-) BQDs used in this study	14
3-2 Three-dimensional models of gas sensing for (a) B_9^- and (b) N/B_9^- BQDs	15
4-1 (a) Side and top views of the optimized structures of B_9^- and N/B_9^- BQDs and (b) DOS of the structures	20
4-2 Side and top views of some optimized B_9^- BQDs for adsorption of (a) NO_2 , (b) CO_2 , (c) CO and (d) NH_3 with perpendicular and parallel orientations	24
4-3 Side and top views of some optimized N/B_9^- BQDs for adsorption of (a) NO_2 , (b) CO_2 , (c) CO and (d) NH_3 with perpendicular and parallel orientations	26
4-4 Calculated DOSs for (a) NO_2 , (b) CO, (c) CO_2 and (d) NH_3 adsorbed on B_9^- and N/B_9^- BQDs structures	29

CHAPTER 1

INTRODUCTION

1.1 Background and Significance

Phetchabun is one of Thailand's important tourist destinations and agricultural cultivation areas. Nowadays, air pollution caused by toxic gases emitted by vehicles on the road, industries, fuel burns, etc., affects human health and cultivation areas in Phetchabun. Numerous hazardous toxic gases are suspended in the air along with various life-sustaining gases, including oxygen, which is necessary for humans, as well as nitrogen and hydrogen, which are crucial for plants to thrive. Toxic gases in the environment mostly include gases such as hydrogen chloride, benzene, dioxin, carbon dioxide, carbon monoxide, or compounds such as asbestos, as well as elements such as mercury, and chromium (Seesaard, Kamjornkittikoon and Wongchoosuk. 2024) etc. Different gases in the environment can act as toxic gases if their concentrations exceed the allowable exposure limits. Moreover, some gases, such as carbon dioxide and carbon monoxide, contribute to the greenhouse effect. To save and protect human health and the environment, innovative technologies are crucial for the detection of these toxic gases. Gas sensors with high performance including fast response, accuracy, high sensitivity and selectivity etc., are essential tools for monitoring and detecting toxic gases the environment. In addition, gas sensors contribute to the fight against climate change by helping monitor greenhouse gas emissions. Development and deployment of gas sensors are critical for safer and cleaner environment.

Recent decades, two-dimensional materials such as graphene, silicene, Mxene, phosphorene and transition metal dichalcogenides have attracted significant interest for various studies of the sensing part of gas sensors (Aufray, Kara, Vizzini, Oughaddou, Léandri,

Ealet and Le Lay 2010 ; Liu, Neal, Zhu, Luo, Xu, Tománek and Ye 2014 ; Seekaew, Kamlue and Wongchoosuk. 2023) due to their unique properties. Unfortunately, these two-dimensional materials own some limitations for gas sensing applications. For instance, the absence of a band gap in graphene makes it difficult to control charge in the sheet (Shukla, Wärma, Jena, Grigoriev and Ahuja. 2017). Borophene is a two-dimensional material made entirely of boron atoms, similar to graphene, but with boron as the main element instead of carbon. Like graphene, borophene has unique properties because of its atomic structures and can potentially be used in various applications due to its exceptional strength, electrical conductivity, and other intriguing characteristics (Zhang, Penev and Yakobson 2017 ; Kaneti, Benu, Xu, Yuliarto, Yamauchi and Golberg 2022 ; Hou, Tai, Liu and Liu. 2022). Boron possesses three valence electrons in $2s^22p^1$ orbitals which can form sp^2 hybridization and the bonding between boron atoms is highly complex with polymorphisms. This complexity leads to various physical and chemical properties (Sabokdast, Horri, Azar, Momeni and Tavakoli. 2021), which distinguish it from other two-dimensional materials like graphene and transition metal dichalcogenides. Owning to a variety of atomic arrangements, there have been reports on theoretical and experimental studies of borophene structures with several stable structures including triangular and hexagonal planar or quasi-planar structure motifs (Yang, Ding and Ni. 2008). Focusing on gas sensing applications, the extraordinary geometries, high surface-to volume ratio and excellent electronic properties of borophene allow it to be used as gas sensors. There have been reports on the adsorption of gas molecules by borophene. For examples, Huang, Murat, Babar, Montes and Schwingenschlögl (2018) calculated adsorption energies, charge transfer and electronic structures of borophene with buckled and line-defective phases for adsorption of NH_3 , NO , NO_2 and CO using density functional theory (DFT). Shukla, Wärma, Jena, Grigoriev and Ahuja (2017) used DFT calculation combined with non-equilibrium Green's function (NEGF) to study adsorption behavior of monolayer

borophene for gas molecules of CO, CO₂, NO, NO₂ and NH₃. These studies showed that borophene could be used as sensing materials for gas sensors to detect toxic gases. However, the mentioned studies focused on gas adsorption of pristine borophene sheets with different structures.

Borophene quantum dots (BQDs) are nanoscale materials that have recently garnered significant interest in the fields of nanotechnology, materials science and nanomedicine. Their sizes are typically in the range of 1-10 nanometers. They exhibit distinct quantum properties influenced by the size and shape of the dots that can be tuned for specific applications (Wang, An, Wang, Sun, Li, Li, Li, Hu and He. 2021). Moreover, their high surface to volume ratio is beneficial for applications like catalysis and sensor development because this high surface area provides more active sites for reactions or interactions. Due to their unique properties, BQDs have been investigated for a wide range of applications including solar cell, biosensors, supercapacitors and catalyst etc. For gas sensing application, research on BQDs based gas sensors for detection of toxic gases is still limited.

In this present research, we theoretically investigate the adsorption behaviors of NO₂, CO₂, CO and NH₃ gas molecules on B₉⁺ wheel structures of pristine and nitrogen functionalized BQDs using self-consistent charge density functional tight-binding (SCC-DFTB) method. We examine adsorption energies, optimal adsorption sites, charge transfer, density of states (DOS) and electronic properties to understand the interaction between these gas molecules and the pristine and nitrogen-functionalized BQDs.

1.2 Objectives

- 1.2.1 To theoretically study the gas sensing properties of borophene quantum dots using three-dimensional models and quantum calculation by self-consistent charge density functional tight-binding (SCC-DFTB) method.

1.2.2 To study the role of nitrogen functionalized on the structures of borophene quantum dots for toxic gas detection.

1.3 Scope of Research

This research will theoretically study the structures of B_9 wheel structures of pristine and nitrogen functionalized borophene quantum dots for toxic gas detection using self-consistent charge density functional tight-binding (SCC-DFTB) method. Toxic gases including NO_2 , CO_2 , CO and NH_3 will be investigated. Adsorption energies, optimal adsorption sites, charge transfer, density of states (DOS) and electronic properties will be calculated to explore and understand the interaction between these gas molecules and the pristine and nitrogen functionalized BQDs. Moreover, effects of nitrogen functionalization on borophene quantum dots for gas detection will be described.

CHAPTER 2

LITERATURE REVIEW

2.1 Borophene and Its Structures and Properties

Borophene is a fascinating two-dimensional (2D) material composed entirely of boron atoms. Unlike graphene, which consists of carbon atoms arranged in a hexagonal lattice, borophene exhibits a variety of unique structures that give it remarkable properties. The different forms of borophene arise from the way that the boron atoms are arranged in the lattice leading to different bonding patterns, symmetry, and electronic behavior. Figure 2-1 shows the different structures of borophene based on arrangement of boron atoms.

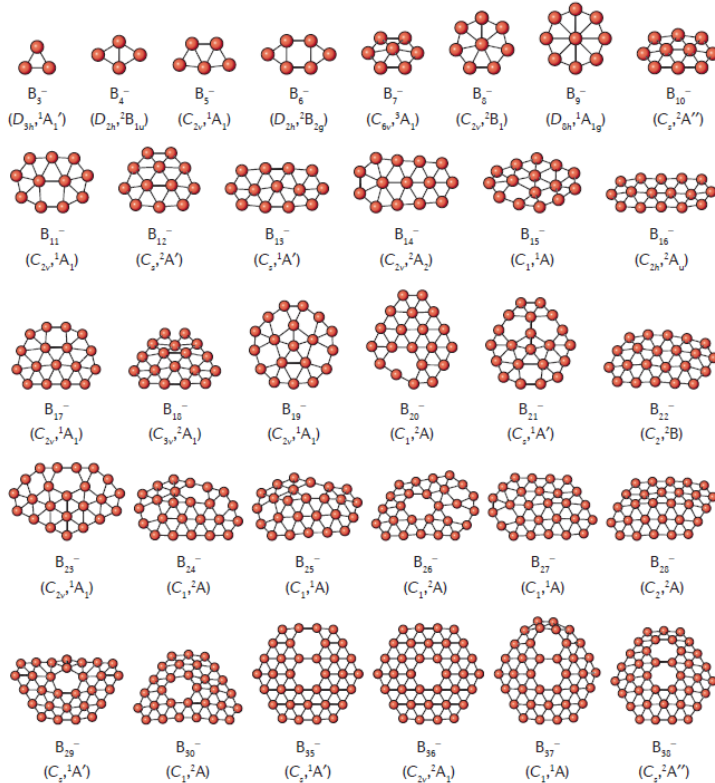


Figure 2-1 Different structures of borophene (Li, Chen, Jian, Chen, Li and Wang. 2017).

Key structural types and properties of borophene are presented as follows:

1. Hexagonal Borophene (β -12 Borophene)

Structure: This is the most well-known and commonly studied structure of borophene. The boron atoms in this structure are arranged in a honeycomb pattern similar to graphene as shown in Figure 2-2. The one key difference is that the atoms are slightly displaced from the perfect two-dimensional plane. The boron atoms form a 12-atom unit cell (hence the name β -12).

Properties: The β -12 structure exhibits a high degree of stability and can have metallic conductivity, which is useful for applications in electronics and energy storage. The boron atoms form strong covalent bonds with one another, giving it mechanical strength. The structure also allows for unique electronic properties due to its distorted honeycomb lattice.

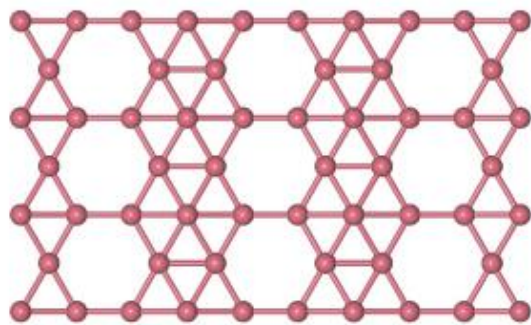


Figure 2-2 The β -12 structure of borophene (Nawal, Banerjee, Reddy and Yamijala. 2024).

2. Honeycomb Borophene

Structure: This structure is similar to the β -12 borophene but with additional boron atoms that modify the bonding, resulting in a more complex lattice. This honeycomb-like

pattern can be regarded as a hybrid of hexagonal borophene with additional atoms as depicted in Figure 2-3.

Properties: The additional boron atoms introduce new electronic states, potentially enhancing its conductivity and catalytic properties. The honeycomb-like structure of this borophene can allow it to mimic certain properties of graphene, making it useful in various nanotechnological applications.

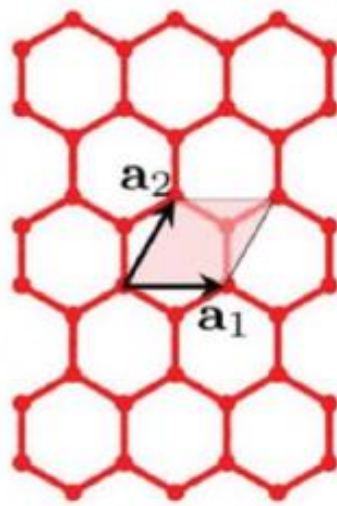


Figure 2-3 Honeycomb borophene (Chand, Kumar and Krishnan. 2021).

3. 2-Pmmn Borophene

Structure: 2-Pmmn borophene represents a unique phase of borophene with a monoclinic symmetry and a distinct atomic arrangement that gives rise to a combination of metallic conductivity, flexibility, and high mechanical strength. Its unique properties open up numerous possibilities for applications in energy storage, catalysis, electronics, and sensing. However, challenges related to its stability in ambient conditions need to be addressed for broader practical use.

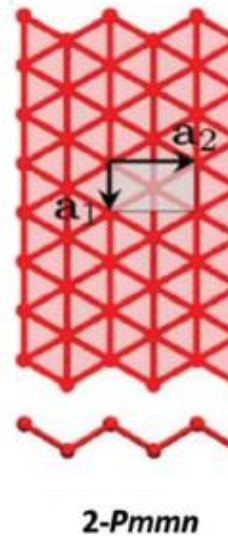


Figure 2-4 2-Pmmn borophene (Chand, Kumar and Krishnan. 2021).

Properties: 2-Pmmn borophene is expected to be metallic, meaning it can conduct electricity. The variation in bond angles and distances within this phase could lead to localized states in the electronic structure, possibly resulting in interesting electronic behavior that could be tuned for specific applications. It exhibits high carrier mobility which depends on the exact atomic arrangement. This characteristic of 2-Pmmn borophene potentially makes it useful for high performance electronics or optoelectronics.

2.2 Borophene Quantum Dots (BQDs)

BQDs are nanoscale fragments of borophene and represent a fascinating subset of this material that harnesses the advantages of quantum confinement. These nanostructures, which have sizes typically in the range of 1 to 10 nm, exhibit enhanced and tunable properties compared to their bulk counterparts, opening new avenues for advanced applications in optoelectronics, sensors, and energy devices.

Structure and Properties: BQDs inherit the structural flexibility and the peculiar bonding characteristics of borophene, which can exhibit a variety of lattice arrangements, from highly ordered honeycomb structures to more distorted or defect-prone configurations. The primary structural feature of borophene quantum dots is their reduced dimensionality, which leads to quantum confinement effects, where the properties of the material change significantly as the size of the structure decreases. The important electronic property of BQDs is:

1. Quantum Confinement: As with many 2D materials, reducing the size of borophene to the quantum dot scale leads to modifications in its electronic band structure. The quantum confinement effect results in discrete electronic energy levels rather than continuous bands, which can drastically affect the electronic and optical properties of the material. The quantum dots could exhibit a bandgap that varies with the size and shape of the quantum dot, providing opportunities to tune their electronic properties for specific applications (Ranjan, Lee, Kumar and Vinu. 2020).
2. Defects and Edge Effects: Borophene is known for its ability to incorporate defects into its structure, and these defects often play a significant role in the properties of borophene quantum dots. The edges of these quantum dots are particularly important because they can introduce localized states in the electronic structure, which can be tuned for use in catalysis or electronic devices. In fact, edge effects in borophene quantum dots might enhance their reactivity and increase their potential as catalysts.
3. Size-Dependent Properties: The properties of borophene quantum dots, such as their electronic bandgap, photoluminescence and mechanical strength, can be tuned by controlling the size and shape of the dots. As the size decreases, the material may transition from metallic to semiconducting behavior, making it

adaptable for a range of optoelectronic applications (Shao, Tai, Hou, Wu, Wu and Liang. 2021).

2.3 Self-Consistent Charge Density Functional Tight-Binding (SCC-DFTB)

SCC-DFTB is a computational method used in chemistry and material science for simulating the electronic structure of molecules and materials. It is a more computationally efficient version of the DFTB (Density Functional Tight Binding) method.

DFTB itself is a simplified version of density functional theory (DFT), which is commonly used in quantum chemistry for calculating the electronic properties of systems. DFTB reduces the computational cost by using a tight-binding approach and approximating the electron-electron interaction in a way that is less computationally demanding than traditional DFT methods. The "Self-Consistent Charge" part of SCC-DFTB means that the charge distribution is updated in a self-consistent manner during the calculations. This allows for more accurate and stable results compared to the standard DFTB method, especially for systems where charge transfer plays a crucial role, such as in molecular simulations or materials science.

Overall, SCC-DFTB is a good compromise between accuracy and computational cost, making it popular for simulating large molecular systems or materials where traditional DFT would be too computationally expensive.

SCC-DFTB has found broad applications in many areas of computational chemistry, materials science, and biology due to its combination of accuracy and efficiency. For materials science, SCC-DFTB has been applied to study bulk materials, nanomaterials and surfaces. It has been particularly useful for simulating materials with large numbers of atoms, such as carbon nanotubes, graphene and semiconductors (Timsorn and Wongchoosuk. 2020).

2.4 Toxic Gases in Environment

Toxic gases in the environment are harmful substances released into the atmosphere that can pose significant risks to human health, animal life and ecosystems as well as agricultural area. These gases may be natural or anthropogenic (human-made) and can come from a variety of sources including industrial activities, transportation, agriculture and natural events like wildfires or volcanic eruptions. Below is an overview of some common toxic gases and their effects on the environment and health:

1. Carbon Monoxide (CO)

Sources: Carbon monoxide is primarily produced by the incomplete combustion of fossil fuels. Common sources include motor vehicles, industrial processes and residential heating systems.

Health Effects: CO is dangerous because it binds to hemoglobin in the blood, reducing oxygen transport to organs and tissues, leading to symptoms like headaches, dizziness, nausea, and, in severe cases, death.

Environmental Impact: Although CO is not directly toxic to plants and animals, it contributes to the formation of ground-level ozone (a component of smog) and can impact air quality.

2. Nitrogen Dioxide (NO₂)

Sources: Nitrogen dioxide is primarily produced from the combustion of fossil fuels, such as in vehicles, power plants, and industrial facilities.

Health Effects: NO₂ can irritate the respiratory system, exacerbate asthma and bronchitis, and increase susceptibility to respiratory infections.

Environmental Impact: NO_2 contributes to the formation of acid rain and ground-level ozone, both of which can harm aquatic ecosystems, soil health, and plant life. It also plays a role in the formation of fine particulate matter (PM2.5), which affects air quality.

3. Ammonia (NH_3)

Sources: Ammonia is primarily released from agricultural activities, particularly livestock waste and the use of fertilizers.

Health Effects: Inhalation of ammonia can cause irritation to the eyes, nose, and respiratory tract. High concentrations can lead to lung damage, and chronic exposure can cause asthma-like symptoms.

Environmental Impact: Ammonia can contribute to eutrophication (nutrient overload) in water bodies, leading to oxygen depletion, which harms aquatic life. It can also cause acidification of soil and water.

4. Methane (CH_4)

Sources: Methane is released during the production and transportation of coal, oil, and natural gas, as well as from livestock, rice paddies, and landfills.

Health Effects: Methane is not toxic in small concentrations, but high levels can displace oxygen in the air, leading to suffocation. It is also a potent greenhouse gas.

Environmental Impact: While methane itself does not directly impact air quality, it is a major contributor to global warming and climate change due to its role as a potent greenhouse gas. It also contributes to the formation of ground-level ozone.

2.5 Gas Sensors

Gas sensors can be broadly classified into several categories based on their working principles. The most common types are:

1. Electrochemical Sensors: These sensors operate based on the electrochemical reaction between the target gas and an electrode. When the gas interacts with the electrode, a current is generated, which is proportional to the gas concentration. Electrochemical sensors are widely used for detecting toxic gases such as carbon monoxide (CO) and nitric oxide (NO) due to their high sensitivity and selectivity.
2. Semiconductor Sensors: Semiconductor gas sensors are based on changes in the electrical resistance of a metal oxide semiconductor when it interacts with target gases. The most common materials used in these sensors include tin oxide (SnO_2) and zinc oxide (ZnO). Semiconductor sensors are popular for detecting a wide range of gases, including methane (CH_4), ammonia (NH_3), and carbon dioxide (CO_2) (Cadena, Riu and Rius. 2007).
3. Infrared (IR) Sensors: These sensors rely on the absorption of infrared light by gas molecules. Different gases absorb infrared radiation at specific wavelengths, allowing for their detection and concentration measurement. IR sensors are particularly useful for detecting gases like CO_2 , methane and volatile organic compounds (VOCs) in both industrial and environmental monitoring (Dinh, Choi, Son and Kim. 2016).
4. Metal Oxide Sensors (MOS): Similar to semiconductor sensors, MOS sensors detect gases by monitoring changes in the conductivity of metal oxide materials (e.g., tin oxide). These sensors are highly sensitive and can be used to detect various gases, including carbon monoxide, hydrogen, and nitrogen dioxide (Cadena, Riu and Rius. 2007).

CHAPTER 3

METHODOLOGY

3.1 Structures of Borophene Quantum Dots (BQDs)

In this study, two structures of BQDs were used for investigation of toxic gas detection including wheel structures of pristine (B_9^-) and nitrogen functionalized (N/B_9^-) BQDs as shown in Figure 3-1. These two structures of BQDs were built using HyperChem Professional software. In case of pristine B_9^- wheel structure of BQDs, a boron atom was placed at the center of a B_8 ring. For nitrogen functionalization, a nitrogen atom was at the center of the B_9^- ring and bonded with nine surrounding boron atoms. It should be noted that this configuration is theoretically feasible because nitrogen can bond to boron forming a stable structure. Then, these structures were optimized and calculated the structural and electronic properties by using SCC-DFTB method.

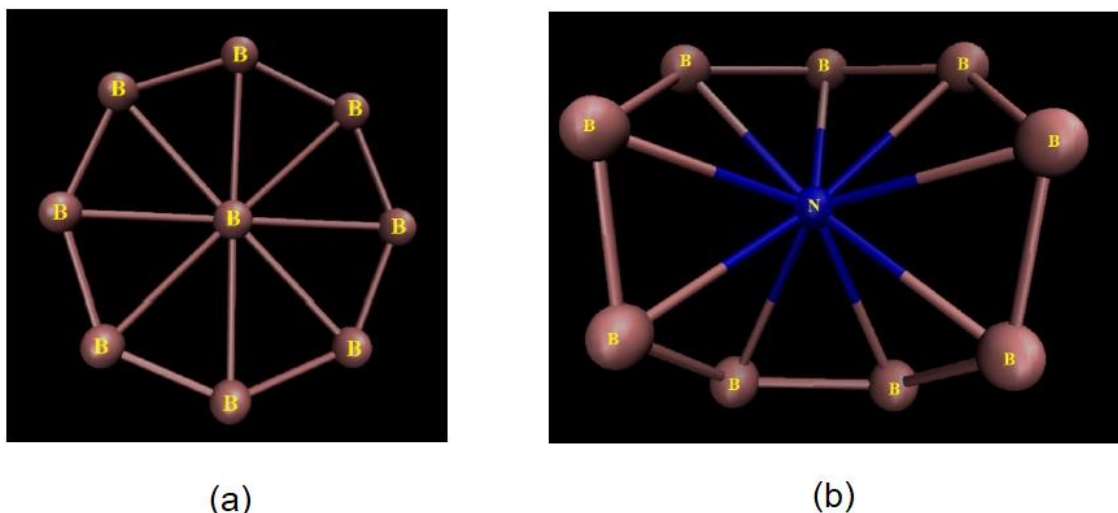


Figure 3-1 Wheel structures of (a) pristine (B_9^-) and (b) nitrogen functionalized (N/B_9^-) BQDs used in this study.

3.2 Three-Dimensional Models of Toxic Gas Sensing

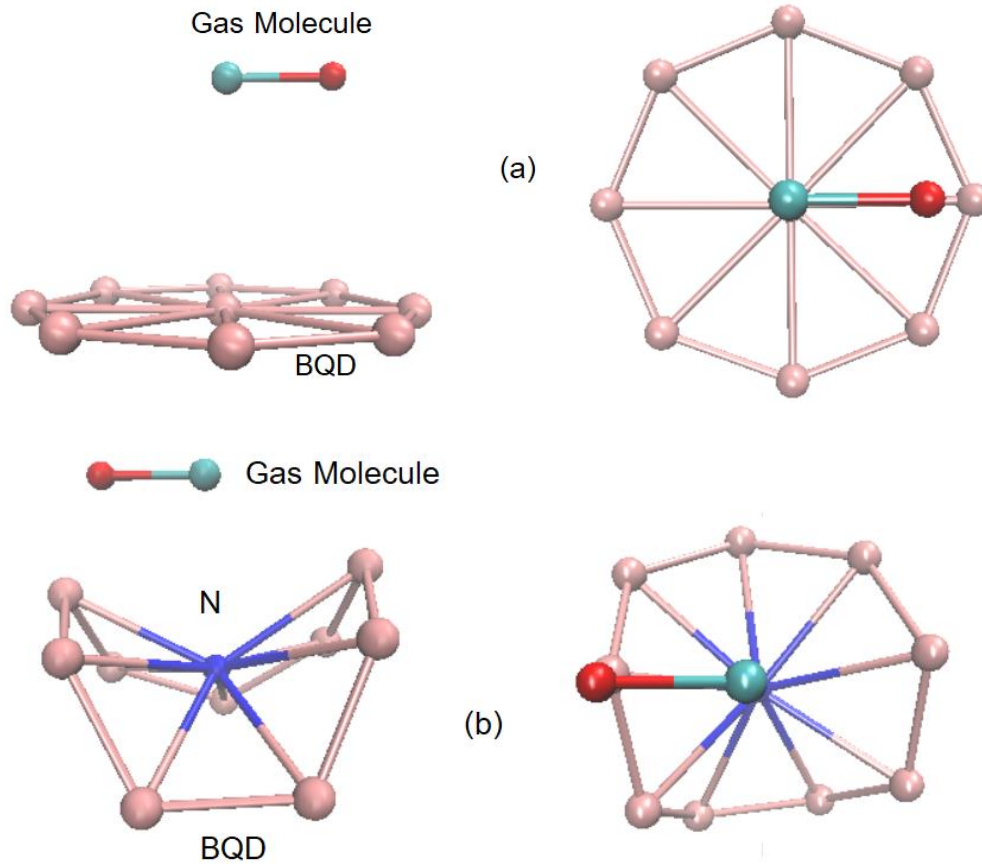


Figure 3-2 Three-dimensional models of gas sensing for (a) B_9^- and (b) N/B_9^- BQDs.

Figure 3-2 shows three-dimensional models for gas sensing. Toxic gas molecules including NO_2 , CO_2 , CO and NH_3 were used to theoretically study gas adsorption behaviors of B_9^- and N/B_9^- BQDs. To study the most favorable adsorption sites, these gas molecules were placed at different distances with orientation configurations (parallel and perpendicular) above the surfaces of B_9^- and N/B_9^- BQDs. Adsorption energies, optimal adsorption sites, charge transfer, density of states (DOS) and electronic properties were calculated to

understand the interaction between these gas molecules and the pristine and nitrogen functionalized BQDs.

3.3 Self-Consistent Charge Density Functional Tight-Binding (SCC-DFTB)

The SCC-DFTB method is an approximate quantum mechanical method that combines the efficiency of the tight-binding approach with the accuracy of density functional theory (DFT). It is derived from second-order expansion of the DFT Kohn-Sham total energy in terms of the charge density fluctuations (Liang, Swanson and Voth. 2014). The SCC-DFTB method starts by constructing the Hamiltonian in a tight-binding form, which includes both the electronic kinetic energy (band structure) and interactions between atoms in the system. The main components of this Hamiltonian are:

One-electron Hamiltonian: Describes the interaction of electrons with atomic nuclei, which is typically derived from Slater-Koster parameters for the overlap matrix and the matrix of electronic integrals.

Two-electron repulsion: This is treated using a screened Coulomb potential, where the electron-electron interaction is approximated.

SCC refers to the iterative procedure used to update the charge distribution. In SCC-DFTB, we calculate the electron density and then iteratively update the charge distribution until convergence. The charge density depends on the electron density at each atomic site. Steps for the SCC procedure are (1) calculate the electron density from the wavefunctions, (2) update the Hamiltonian using the new charge density, (3) solve for the electronic structure (i.e., eigenvalues and eigenvectors) of the system using the updated Hamiltonian, (4) update the charge distribution based on the new electronic structure and (5) repeat until the charge density converges to a self-consistent solution.

Based on Kohn-Sham orbitals, the total energy for the SCC-DFTB method is expressed as (Timsorn and Wongchoosuk. 2020):

$$E_{\text{tot}}^{\text{SCC-DFTB}} = \sum_i \langle \phi_i | \hat{H}_0 | \phi_i \rangle + \frac{1}{2} \sum_{A,B} \gamma_{AB} \Delta q_A \Delta q_B + E_{\text{rep}} \quad (1)$$

where ϕ_i are the Kohn-Sham orbitals, \hat{H}_0 is unperturbed Hamiltonian, Δq_A and Δq_B are the induced charges on the atoms A and B, respectively, γ_{AB} is the second derivative with respect to its total charges (Coulombic-like interaction potential) and E_{rep} denotes repulsive potential for the pair of atoms A and B.

The matsci-0-3 parameter set was used for calculation in O-N-C-B-H system. In addition, the matsci-0-3 parameter set well describes the interaction of covalent organic system, especially small organic molecules containing nitrogen, oxygen, carbon and hydrogen (Elstner, Porezag, Jungnickel, Elsner, Haugk, Frauenheim, Suhai and Seifert. 1998). To investigate the adsorption behaviors of NO_2 , CO_2 , CO and NH_3 on the surfaces of B_9^- and N/B_9^- BQDs, adsorption strengths between the structures and these gas molecules are described in the term of adsorption energies (E_{ad}). The adsorption energy is calculated as the following equation:

$$E_{\text{ad}} = E_{\text{tot}}(\text{BQDs} + \text{gas molecules}) - E_{\text{tot}}(\text{BQDs}) - E_{\text{tot}}(\text{gas molecules}) \quad (2)$$

where $E_{\text{tot}}(\text{BQDs} + \text{gas molecules})$, $E_{\text{tot}}(\text{BQDs})$ and $E_{\text{tot}}(\text{gas molecules})$ are the total energies of B_9^- or N/B_9^- BQDs with gas molecules, BQDs and gas molecules, respectively. A negative value of E_{ad} indicates that gas molecules are adsorbed and more negative values are more favorable adsorption sites.

To study charge transfers from/to gas molecules resulting from the adsorption, net charge transfer is defined as the charge difference of gas molecules before and after

adsorption (Wang, Zhu and Zhang. 2008). The net charge transfer (Q) is obtained from equation (3):

$$Q = Q(\text{BQDs} + \text{gas molecules}) - Q(\text{gas molecules}) \quad (3)$$

where $Q(\text{BQDs} + \text{gas molecules})$ and $Q(\text{gas molecules})$ are the charges of gas molecules adsorbed on the surfaces of BQDs structures and isolated gas molecules, respectively.

Total density of states (DOS) was calculated to analyze the influence of gas molecule adsorption on the electronic properties of BQDs. The k -point sampling density was set to $5 \times 5 \times 1$ for the DOS studies. It should be noted that DOS is a key concept in the electronic properties of materials. It describes the number of electronic states available per unit energy at each energy level for a material. More specifically, the DOS provides insight into how many electron states can be occupied at a given energy in a solid. For gas sensing, DOS plays a crucial role in understanding and optimizing the gas sensing properties of materials. Electronic properties, which are directly influenced by the DOS, affect how materials interact with gas molecules. These are how DOS impacts gas sensing:

1. Surface Interaction

In gas sensors, the interaction between gas molecules and the sensor materials typically occurs on the surfaces. When gas molecules adsorb onto the surfaces, they can donate or accept electrons causing a change in the electronic states near the surface. The availability of electronic states (as described by the DOS) at particular energy levels influences how easily gas molecules can transfer charge to or from the materials.

2. Change in Conductivity

For semiconductor-based gas sensors (e.g., SnO_2 , ZnO , or graphene), the adsorption of gas molecules affects charge carrier density of materials. For n-type semiconductors, gas molecules that accept electrons (like oxygen or NO_2) reduce the

electron density and increase resistance, while gases that donate electrons (like H₂ or CO) increase the electron density and decrease resistance. The total DOS, particularly around the Fermi level, affects how the charge density changes and how significant the conductivity variation will be upon gas adsorption.

3. Band Structure and Sensitivity

The DOS near the Fermi level is critical for determining how the material will respond to gas molecules. A material with a higher DOS at the Fermi level can provide more available states for electron exchange, potentially enhancing gas sensitivity. For example, materials like graphene and carbon nanotubes are sensitive to gas adsorption due to their high DOS near the Fermi level allowing even small changes in adsorbed gases to significantly impact their electronic properties.

4. Selectivity

The selectivity of a gas sensor, the ability to detect one type of gas in the presence of others, is partly determined by the specific DOS distribution of the sensor materials. Different gases may interact more strongly with certain energy states and the DOS can help predict which gases will have a stronger or weaker effect on the conductivity or surface charge of materials.

5. Charge Transfer and Energy Levels

Gas molecules typically interact with the sensor materials by transferring charge. The amount of charge transfer depends on the alignment of the gas molecule energy levels with the DOS of the materials. For gases to donate or accept electrons, there must be available states in the DOS at energies matching the molecular energy levels (e.g., the HOMO or LUMO of the gas molecules).

CHAPTER 4

RESULTS AND DISCUSSION

4.1 Structural and Electronic Properties of B_9^- and N/B_9^- BQDs

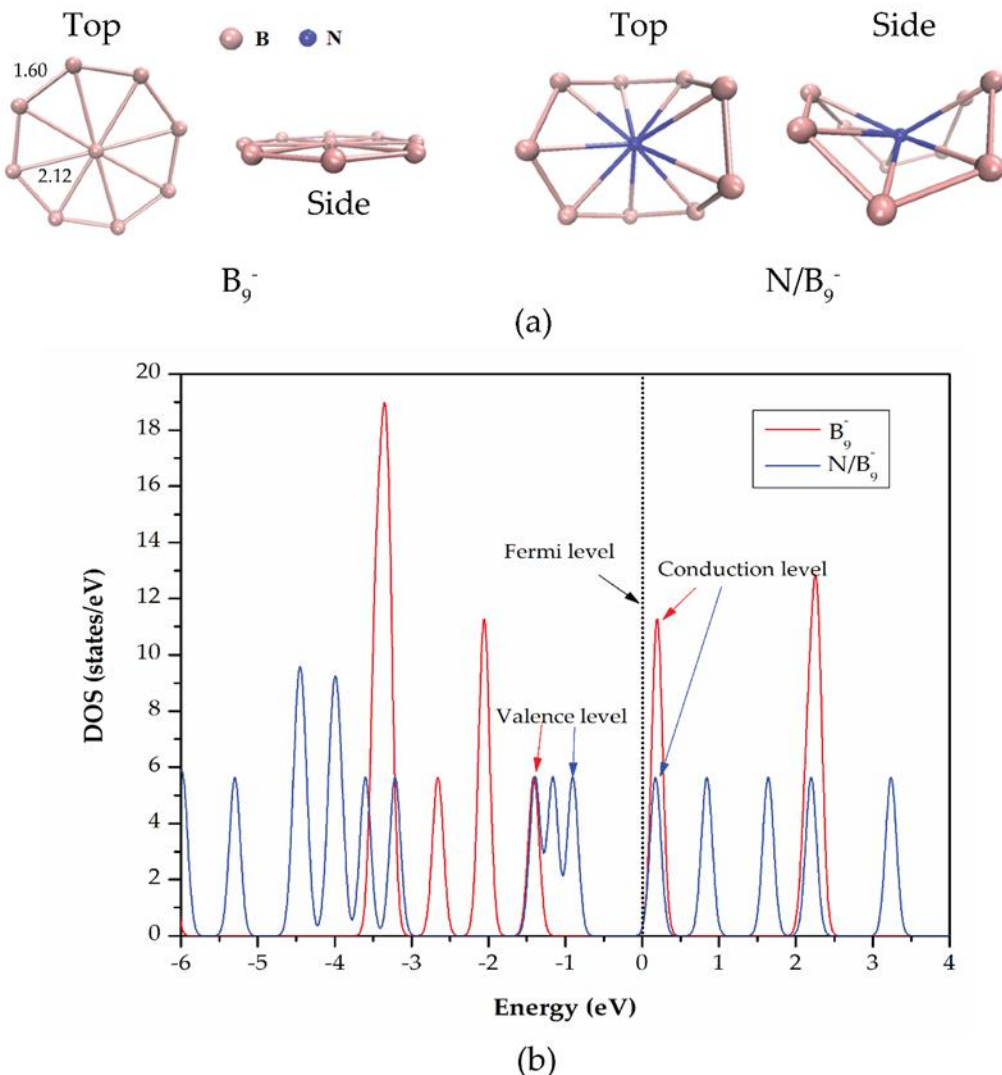


Figure 4-1 (a) Side and top views of the optimized structures of B_9^- and N/B_9^- BQDs and (b) DOS of the structures.

Figure 4-1(a) shows the optimized structures of B_9^- and N/B_9^- BQDs with side and top views. These structures were optimized to obtain the most stable structure. During the optimization process, the initial geometries of the BQD structures were input into the SCC-DFTB framework. The energy minimization was performed iteratively by adjusting atomic positions with the forces on each atom being calculated at each step. The optimization continued until the system reached a stable configuration where the forces on the atoms were below a predefined threshold and the total energy converged.

For the B_9^- BQDs, it was found that the bond lengths between the central boron atom and each boron atom of the B_8 ring are $\sim 2.12 \text{ \AA}$. The structural diameter and the bond lengths between boron atoms on the B_8 ring side are $\sim 4.22 \text{ \AA}$ and $\sim 1.60 \text{ \AA}$, respectively. The side view reveals that the structure of B_9^- BQDs is relatively flat. The central boron atom contributes all three valence electrons to the delocalized bonding. The boron atoms in the ring side contribute their two valence electrons to two-center, two-electron (2c-2e) boron-boron bonds of the ring while the remaining valence electron participates in delocalized σ and π bonding with the central boron atom. For nitrogen functionalization, a nitrogen atom (blue color) was placed at the center of the ring. It can be obviously seen that the structural distortion occurred. The structure is buckled where some boron atoms move inward or outward with respect to the central nitrogen atom. The distortion arises from the inherent nature of borophene with boron atoms forming triangles or hexagons in which nitrogen doping can induce structural distortions because nitrogen has a stronger bonding capability than boron. This can introduce new electronic states and shift the overall energy distribution of the system. The bond lengths between the boron atoms on the ring side and the central nitrogen atom are changed to be in the range of $1.88 - 2.00 \text{ \AA}$.

To study electronic properties of B_9^- and N/B_9^- BQDs, we calculated energy gap (E_g), E_{LUMO} , E_{HOMO} , Fermi energy (E_F) and DOS as presented in Table 4-1 and Figure 4-1(b). It was

found that E_g decreases significantly from 2.72 eV to 0.68 eV after nitrogen functionalization. The large decrease of E_g results from a change in energy levels of the conduction band edge (E_{LUMO}) and the valence band edge (E_{HOMO}) as shown in Table 4-1. The conduction band edge shifts downward and the valence band edge shifts upward. This result reveals that nitrogen functionalization at the center of the boron ring introduces impurity states within the band structure of B_9^- BQDs. The interaction between these impurity states and an additional electron, which occupy in the conduction band or near the conduction band edge in the B_9^- structure, modifies the energy levels near the Fermi level resulting in the reduced energy gap. Figure 4-1(b) shows the calculated DOS of B_9^- and N/B_9^- BQDs. It should be noted that the DOS describes the distribution of electronic states as a function of energy. It can be clearly seen that new DOS peaks (blue lines) around the vicinity of the Fermi level appeared after nitrogen functionalization. This confirms that nitrogen functionalization creates new localized states due to the difference in electronic configuration of nitrogen atoms compared to boron atoms which indicates the presence of electrons or holes. The E_g values from Table 4-1 correspond well with those shown in Fig. 4-1(b).

Table 4-1. Electronic parameter of B_9^- and N/B_9^- BQDs.

Structure	E_{HOMO} (eV)	E_{LUMO} (eV)	E_F (eV)	E_g (eV)
B_9^-	-6.18	-3.46	-6.15	2.72
N/B_9^-	-5.98	-5.30	-5.64	0.68

4.2 Adsorption of NO_2 , CO_2 , CO and NH_3 gas molecules on B_9^- BQDs

To investigate the adsorption behavior of B_9^- BQDs for detection of NO_2 , CO_2 , CO and NH_3 gas molecules, the different adsorption structures were constructed and fully optimized. Each gas molecule was placed on the top of the B_9^- BQD structures with both parallel and perpendicular orientations. Each atom of these gas molecules was pointed toward a boron atom of the structures including N-B, C-B, O-B and H-B to find the most favorable adsorption sites. Figure 4-2 shows side and top views of some optimized B_9^- BQD structures with gas molecules on the top of the structures in parallel and perpendicular orientations. The typical calculated adsorption parameters are summarized in Table 4-2. Based on overview of the calculated E_{ad} values, it is found that the highest to lowest E_{ad} values are found for NO_2 , CO, CO_2 and NH_3 , respectively. In each case, the E_{ad} values are higher than adsorption energies of borophene sheets for these toxic gases. This result reveals that quantum confinement effects and high surface to volume ratio of the BQDs improve the adsorption performance for gas sensing. For charge transfer calculation, the most values of charge transfer are found to be positive. Also, large charge transfer is found for all gas molecules. The positive (negative) sign of charge transfer shows that gas molecules accept (donate) electrons.

To consider the adsorption sites of each gas molecule, the most favorable adsorption sites for NO_2 , CO, CO_2 and NH_3 were identified as B-O (perpendicular), B-C (parallel), B-C (parallel) and B-N (perpendicular), respectively. Interestingly, both CO and CO_2 prefer B-C adsorption sites with parallel orientation. In case of energy gap, it can be obviously seen that the energy gap decreases for all adsorption sites of all gas molecules which suggests that conductivity of the B_9^- BQDs increases after gas adsorption. Based on the results of Table 4-2, high adsorption energies, large charge transfer and short interaction distances reveal that the interaction between gas molecules and the B_9^- BQDs is a result of chemisorption (Shukla, Wärma, Jena, Grigoriev and Ahuja. 2017).

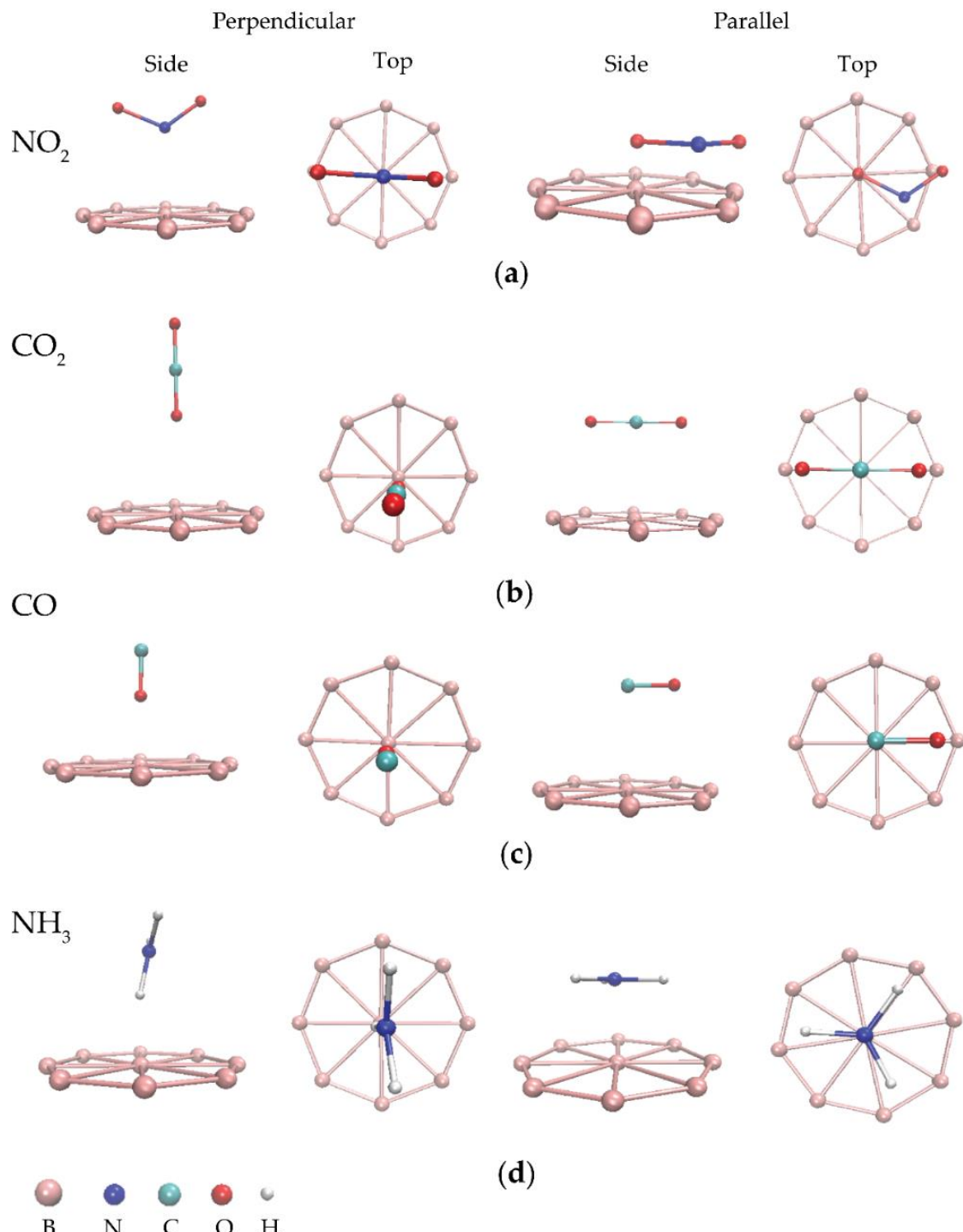


Figure 4-2 Side and top views of some optimized B_9^- BQDs for adsorption of (a) NO_2 , (b) CO_2 , (c) CO and (d) NH_3 with perpendicular and parallel orientations.

Table 4-2. Typical calculated adsorption parameters for each gas molecule adsorbed on the B_9^- BQD structures.

System	Orientation	Adsorption site	Distance (Å)	E_{ad} (eV)	Q (e)	E_{HOMO} (eV)	E_{LUMO} (eV)	E_g (eV)
B_9^- - NO_2	parallel	B-N	1.23	-5.80	0.273	-5.81	-4.31	1.50
		B-O	2.25	-4.39	0.218	-5.94	-4.99	0.95
	perpendicular	B-N	2.97	-4.39	0.218	-5.94	-4.99	0.95
		B-O	3.00	-6.52	0.166	-5.59	-4.56	1.03
B_9^- - CO	parallel	B-C	1.01	-8.47	-0.164	-5.42	-4.41	1.01
		B-O	1.12	-6.82	-0.317	-6.12	-5.30	0.82
	perpendicular	B-C	2.41	-2.04	0.370	-5.61	-3.44	2.17
		B-O	1.04	-0.72	0.341	-5.65	-3.39	2.26
B_9^- - CO_2	parallel	B-C	1.75	-6.66	0.131	-5.26	-4.49	0.77
		B-O	1.72	-3.93	-0.027	-5.83	-4.61	1.22
	perpendicular	B-C	2.20	-0.61	0.470	-5.07	-2.63	2.44
		B-O	1.34	-0.60	0.467	-5.09	-2.88	2.21
B_9^- - NH_3	parallel	B-N	3.00	-1.77	0.421	-5.16	-2.77	2.39
		B-H	3.58	-1.78	0.420	-5.14	-2.90	2.24
	perpendicular	B-N	1.00	-4.06	0.083	-5.22	-4.21	1.01
		B-H	2.50	-1.78	0.420	-5.14	-2.90	2.24

4.3 Adsorption of NO_2 , CO_2 , CO and NH_3 gas molecules on N/B_9^- BQDs

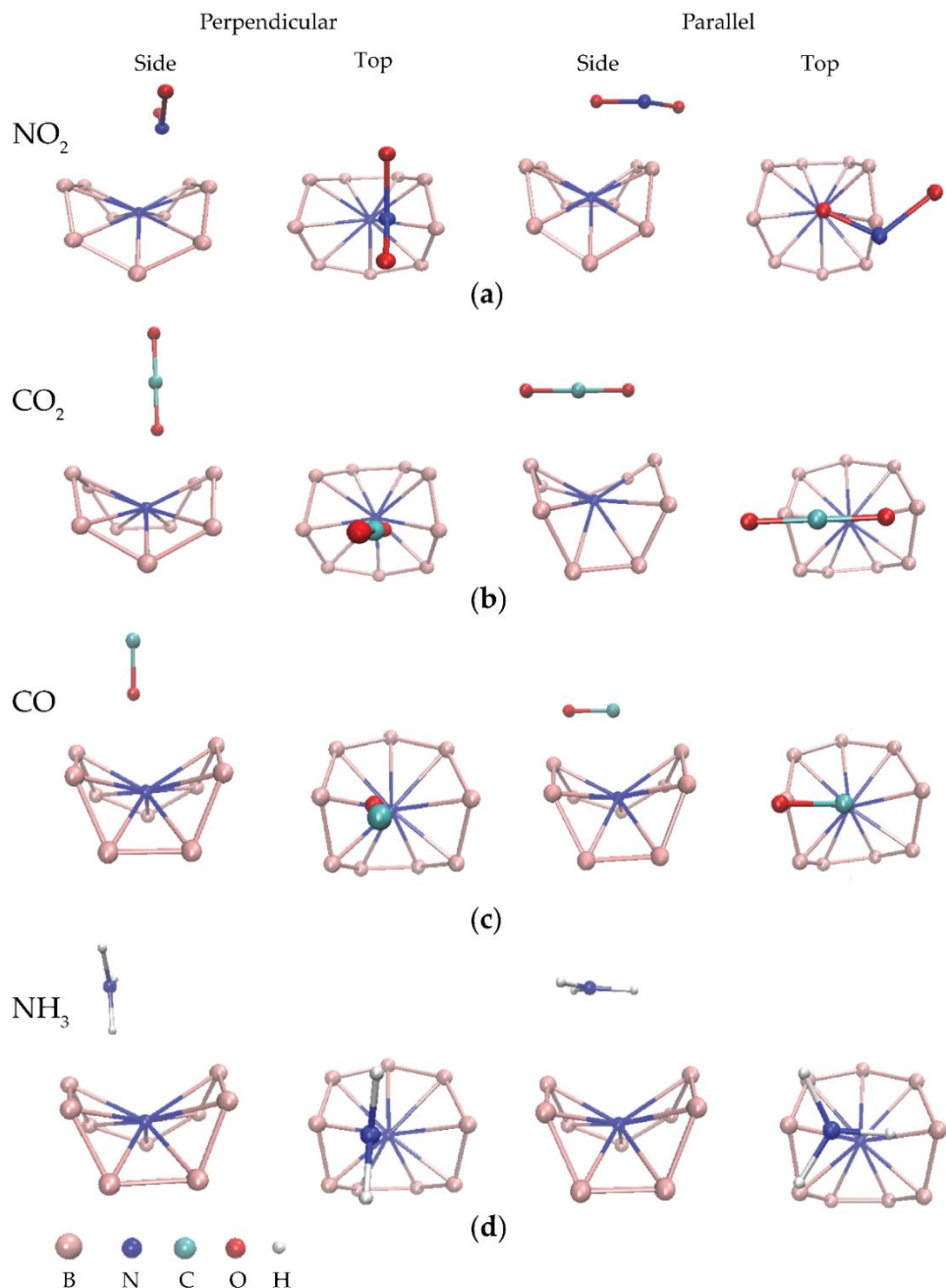


Figure 4-3 Side and top views of some optimized N/B_9^- BQDs for adsorption of (a) NO_2 , (b) CO_2 , (c) CO and (d) NH_3 with perpendicular and parallel orientations.

Figure 4-3 displays some optimized N/B_9^- BQD structures for adsorption of NO_2 , CO_2 , CO , and NH_3 gas molecules at different interaction distances. The calculated adsorption parameters are presented in Table 4-3. Each atom of gas molecules was placed on the top of the N/B_9^- BQD structures pointing to the nitrogen atom with parallel and perpendicular orientation. According to the results of Table 4-3, the results shows that the E_{ad} values of the N/B_9^- BQDs for all gas molecules at all adsorption sites obviously increased in comparison with the E_{ad} values of the B_9^- BQDs. The favorable adsorption sites for NO_2 , CO and CO_2 are parallel orientation except for NH_3 which preferred perpendicular orientation. The highest E_{ad} values of CO_2 , CO , NO_2 and NH_3 at their most favorable adsorption sites are -16.57, -12.08, -11.64 and -7.22 eV, respectively. There are two reasons that can describe this result. First, the functionalized nitrogen atom introduces impurity states leading to strong interaction. Second, the buckling of the N/B_9^- BQDs allows gas atoms bonding with more than one surrounding boron atoms. Looking at charge transfer, it is found that the most charge transfer is positive and lower than that of the B_9^- BQDs. This demonstrates that the trend in charge transfer of each gas molecule is still from the structures to gas molecules. It is attributed that the lower charge transfer results from strong interaction (high E_{ad} values), localized electronic states from impurities and buckled surface of the N/B_9^- BQDs, which affects pathway of charge transfer. The interaction distances for all adsorption sites are in the range of chemical bonding indicating chemisorption.

For energy gap, the trend in slightly increases energy gap of the N/B_9^- BQDs after adsorption of NO_2 , CO_2 and NH_3 whereas the energy gap of CO adsorbs on the structure tend to be decreased. We will explain this result in the section of DOS. A comparison of adsorption energies with other two-dimensional materials such as graphene, for instance, exhibited weak adsorption energies for NO_2 , CO_2 , CO and NH_3 gas molecules. The adsorption energies of NO_2 , CO and NH_3 gas molecules on borophene sheets were found to be -1.75, -

1.24 and -1.45 eV, respectively (Huang, Murat, Babar, Montes and Schwingenschlögl. 2018). In case of MoS_2 , the adsorption energies were -0.44 and -0.33 eV for CO and CO_2 , respectively. Based on the results, nitrogen functionalization at the center of the B_9^- BQD ring could improve the adsorption behavior of B_9^- BQDs for NO_2 , CO_2 , CO and NH_3 gas molecules.

Table 4-3. Typical calculated adsorption parameters for each gas molecule absorbed on the N/B_9^- BQD structures.

System	Orientation	Adsorption site	Distance (\AA)	E_{ad} (eV)	Q (e)	E_{HOMO} (eV)	E_{LUMO} (eV)	E_g (eV)
N/B_9^- - NO_2	parallel	N-N	1.00	-11.64	0.021	-5.04	-4.55	0.49
		N-O	2.52	-8.67	0.036	-5.24	-4.29	0.95
	perpendicular	N-N	1.15	-6.99	0.014	-5.35	-4.52	0.83
		N-O	3.10	-8.67	0.036	-5.24	-4.29	0.95
N/B_9^- -CO	parallel	N-C	1.15	-12.08	0.105	-5.17	-4.56	0.61
		N-O	1.34	-7.86	-0.117	-5.42	-4.82	0.60
	perpendicular	N-C	1.65	-4.28	0.166	-6.03	-5.71	0.32
		N-O	1.80	-4.60	0.147	-5.62	-4.79	0.83
N/B_9^- - CO_2	parallel	N-C	1.25	-16.57	-0.086	-5.92	-3.88	2.04
		N-O	1.20	-16.11	-0.466	-5.80	-4.58	1.22
	perpendicular	N-C	2.51	-6.57	0.201	-4.98	-4.18	0.80
		N-O	1.00	-3.23	0.115	-5.80	-4.90	0.90
N/B_9^- - NH_3	parallel	N-H	1.02	-6.34	0.121	-5.92	-4.81	1.11
		N-N	1.14	-6.70	0.039	-5.90	-5.00	0.90
	perpendicular	N-H	1.57	-7.22	0.116	-5.41	-4.19	1.22
		N-N	1.05	-6.80	-0.049	-5.90	-4.86	1.04

4.4 Total Densities of State (DOS)

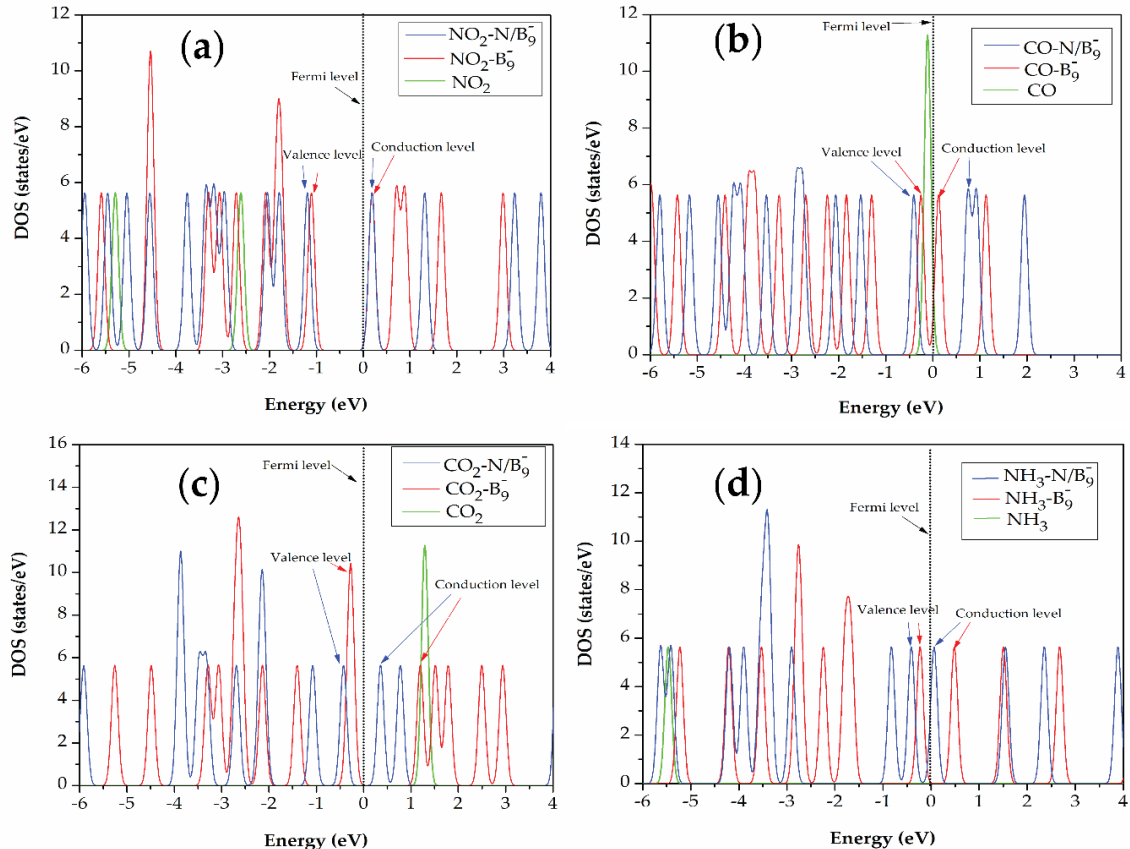


Figure 4-4 Calculated DOSs for (a) NO_2 , (b) CO , (c) CO_2 and (d) NH_3 adsorbed on B_9^- and N/B_9^- BQDs structures. The Fermi level is set to zero with dashed vertical lines.

DOS calculations were performed to gain insights into the interactions between gas molecules and both B_9^- and N/B_9^- BQDs structures. Figure 4-4 demonstrates the calculated DOS of the most favorable adsorption sites for each gas molecule. It was observed that sharp DOS peaks appeared near the Fermi level for all gas molecules adsorbed on the N/B_9^- BQDs indicating strong bonding which corresponds to higher adsorption energies than the B_9^- BQDs with gas molecules. In both cases, DOS peaks near the Fermi level suggest charge transfer

from the BQDs to the gas molecules. Among all these gases, only CO contributes states near the Fermi level, specifically at the top of valence band, which might improve the conductivity. This confirms the decreasing energy gap in case of CO adsorbed on the N/B_9^- BQDs, which is the reason for the section 4.3. To consider in details of each case as shown in Figure 4-4 (a-d), new local states appeared near the conduction band edge for NO_2 , CO_2 and NH_3 on N/B_9^- BQDs, while in case of $\text{CO-N}/\text{B}_9^-$ BQD, a new local state appeared below the Fermi level at -0.4 eV. This suggests the existence of localized states from the impurities interacting with gas molecules.

CHAPTER 5

CONCLUSION

The study investigated the adsorption behaviors of NO_2 , CO_2 , CO, and NH_3 gases on both pristine and nitrogen-functionalized borophene quantum dots (B_9^- and N/B_9^- BQDs) using self-consistent charge density functional tight-binding (SCC-DFTB) methods. Structural geometries, the most favorable adsorption sites and electronic properties were investigated. The results showed that nitrogen functionalization at the center of B_9^- BQDs structures significantly enhanced the adsorption performance of B_9^- BQDs for all the tested gases leading to stronger adsorption energies and larger charge transfers. Based on the adsorption results, the adsorption energies of these structures were found to be higher than those of borophene sheets. Additionally, the adsorption energies of the N/B_9^- BQDs were higher than those of the B_9^- BQDs. The B_9^- BQDs favored NO_2 adsorption while the N/B_9^- BQDs favored CO_2 with parallel orientation.

In case of DOS analysis, DOS calculations provided valuable insights into the interactions between gas molecules and both B_9^- and N/B_9^- BQDs. For all gas molecules adsorbed on N/B_9^- BQDs, sharp DOS peaks were observed near the Fermi level that indicated strong gas adsorption. This strong interaction was also reflected in the higher adsorption energies compared to pristine B_9^- BQDs. In particular, carbon monoxide (CO) was the only gas that introduced new states near the Fermi level in the valence band suggesting enhanced conductivity of the materials after adsorption. This finding aligns with the observed reduction in the energy gap in the case of CO adsorption. Additionally, localized states that appeared near the conduction band edge for NO_2 , CO_2 , and NH_3 on N/B_9^- BQDs confirm strong interactions due to nitrogen functionalization and impurity states. These localized states

contribute to the charge transfer mechanism between the gas molecules and the BQDs, reinforcing the potential of nitrogen-functionalized BQDs in toxic gas sensing applications.

These findings suggest that BQDs with nitrogen functionalization show strong potential for applications in toxic gas sensors due to their high sensitivity, selectivity, and tunable properties. In addition, the interaction between BQDs and the gas molecules was found to be chemisorption, which indicates the suitability of these materials for environmental monitoring and protection.

REFERENCES

Seesaard, T. *et al.* "A Comprehensive Review on Advancements in Sensors for Air Pollution Applications." *Sci. Total Environ.* 951(2024) : 175696.

Seekaew, Y. *et al.* "Room-Temperature Ammonia Gas Sensor Based on $Ti_3C_2T_x$ MXene/Graphene Oxide/CuO/ZnO Nanocomposite." *ACS Appl. Nano Mater.* 6(2023) : 9008–9020.

Aufray, B. *et al.* "Graphene-Like Silicon Nanoribbons on Ag(110): a Possible Formation of Silicene." *Appl. Phys. Lett.* (96)2010 : 183102.

Liu, H. *et al.* "Phosphorene: an Unexplored 2D Semiconductor with a High Hole Mobility." *ACS Nano.* (8)2014 : 4033-4041.

Shukla, V. *et al.* "Toward the Realization of 2D Borophene Based Gas Sensor." *J. Phys. Chem. C.* 121(2017) : 26869-26876.

Kaneti, Y.V. *et al.* "Borophene: Two-Dimensional Boron Monolayer: Synthesis, Properties, and Potential Applications." *Chem. Rev.* (122) 2022 : 1000-1051.

Hou, C. *et al.* "Borophene gas sensor." *Nano Res.* 15(3)(2022) : 2537-2544.

Zhang, Z.H. *et al.* "Two-Dimensional Boron: Structures, Properties and Applications." *Chem. Soc. Rev.* 46(2017) : 6746-6763.

Sabokdast, S. *et al.* "Detection of Nucleobases on Borophene Nanosheet: a DFT Investigation." *Bioelectrochemistry.* 138(2021) : 107721.

Yang, X. *et al.* "Ab initio Prediction of Stable Boron Sheets and Boron Nanotubes: Structure, Stability, and Electronic Properties." *Phys. Rev. B.* 77(2008) : 041402.

Huang, C.S. *et al.* "Adsorption of the Gas Molecules NH_3 , NO, NO_2 , and CO on Borophene." *J. Phys. Chem. C.* 122(2018) : 14665-14670.

Wang, H. *et al.* "Crystalline Borophene Quantum Dots and Their Derivative Boron Nanospheres." **Mater. Adv.** 2(2021) : 3269-3273.

Li, W.L. *et al.* "From Planar Boron Clusters to Borophenes and Metalloboroophenes." **Nat. Rev. Chem.** 1(2017) : 1.

Narwal, A. *et al.* "AB-Stacked Bilayer β_{12} -Borophene as a Promising Anode Material for Alkali Metal-Ion Batteries." **J. Energy Storage.** 102(2024) : 114023.

Chand, H. *et al.* "Borophene and Boron-Based Nanosheets: Recent Advances in Synthesis Strategies and Applications in the Field of Environment and Energy." **Adv. Mater. Interfaces.** 8(2021) : 2100045.

Shao, W. *et al.* "Borophene-Functionalized Magnetic Nanoparticles: Synthesis and Memory Device Application." **ACS Appl. Electron. Mater.** 3(2021) : 1133-1141.

Ranjan, P. *et.al.* "Borophene: New Sensation in Flatland." **Adv. Mater.** 1(2020) : 2000531.

Timsorn, K. and Wongchoosuk, C. "Adsorption of NO_2 , HCN, HCHO and CO on Pristine and Amine Functionalized Boron Nitride Nanotubes by Self-Consistent Charge Density Functional Tight-Binding Method." **Mater. Res. Express.** 7(2020) : 055005.

Cadena, G.J. et al. "Gas Sensors Based on Nanostructures Materials." **Analyst.** 132(2007) : 1083-1099.

Dinh, T.V. *et al.* "A Review on Non-dispersive Infrared Gas Sensors: Improvement of Sensor Detection Limit and Interference Correction." **Sens. Actuators B: Chem.** 231(2016) : 529-538.

Liang, R. *et al.* "Benchmark Study of the SCC-DFTB Approach for a Biomolecular Proton Channel." **J. Chem. Theory Comput.** 10(1)(2014) : 451-462.

Elstner, M. *et al.* "Self-Consistent-Charge Density-Functional Tight-Binding Method for Simulation of Complex Materials Properties." *Phys. Rev. B.* 58(1998) : 7260.

Wang, R. *et al.* "Adsorption of Formaldehyde Molecule on the Pristine and Silicon-Doped Boron Nitride Nanotubes." *Chem. Phys. Lett.* 467(2008) : 131-135.

CURRICULUM VITAE

2. K. Timsorn, and C. Wongchoosuk. 2019. "Inkjet printing of room-temperature gas sensors for identification of formalin contamination in squids", *Journal of Materials Science: Materials in Electronics* 30: 4782-4791.
3. K. Timsorn, Y. Lorjaroenphon and C. Wongchoosuk. 2017. "Identification of adulteration in uncooked Jasmine rice by a portable low-cost artificial olfactory system". *Measurement* 108: 67-76.
4. P. Traiwatcharanon, K. Timsorn and C. Wongchoosuk. "Flexible room temperature resistive humidity sensor based on silver nanoparticles". *Materials Research Express* 4 (2017): 1-10.
5. K. Timsorn, T. Thoopboochagorn, N. Lertwattanasakul and C. Wongchoosuk. 2016. "Evaluation of bacterial population on chicken meats using a briefcase electronic nose", *Biosystems Engineering* 151: 116-125.
6. P. Traiwatcharanon, K. Timsorn and C. Wongchoosuk. 2016. "Effect of pH on the green synthesis of silver nanoparticles through reduction with Pistia stratiotes L. extract", *Advanced Materials Research* 1131: 223-226.
7. K. Timsorn, C. Wongchoosuk, P. Wattuya, S. Promdaen and S. Sittichat. 2014. "Discrimination of chicken freshness

using electronic nose combined with PCA and ANN”, *IEEE*:
1-4.

7. Awards

รางวัลผลงานประดิษฐ์คิดค้น ประจำปี ๒๕๖๑ รางวัลประกาศ
เกียรติคุณ เรื่อง ปืนตรวจวัดการปนเปื้อนสารฟอร์มาลีนในอาหาร
แบบพกพาได้ จากสำนักงานคณะกรรมการวิจัยแห่งชาติ (วช)